Protective Effects of *Mundongcheongpye-eum* on Lung Injury Induced by Elastase

Tae Heung Nam, Yang Chun Park*

Division of Respiratory System, Department of Internal Medicine, College of Oriental Medicine, Daejeon University

This study aimed to evaluate the protective effects of *Mundongcheongpye-eum* (MCE) on elastase-induced lung injury. The extract of MCE was treated to A549 cells and elastase-induced lung injury mice model. Then, various parameters such as cell-based cyto-protective activity and histopathological finding were analyzed. MCE showed a protective effect on elastase-induced cytotoxicity in A549 cells. This effect was correlated with analysis for caspase 3 levels, collagen and elastin contents, protein level of cyclin B1, Cdc2, and Erk1/2, and gene expression of TNF-α and IL-1β in A549 cells. MCE treatment also revealed the protective effect on elastase-induced lung injury in mice model. This effect was evidenced via histopathological finding including immunofluence stains against elastin, collagen, caspase 3, and protein level of cyclin B1, Cdc2, and Erk1/2 in lung tissue. These data suggest that MCE has a pharmaceutical properties on lung injury. This study would provide an scientific evidence for the efficacy of MCE for clinical application to patients with chronic obstructive pulmonary disease.

Key words : *Mundongcheongpye-eum (Mendongqingfei-yin)*, Chronic obstructive pulmonary disease, Elastase, A549 cell, Lung tissue

Introduction

Chronic obstructive pulmonary disease (COPD) is one of the major diseases marking high incidence rate in Korea (7.8%) with mortality rate of 14.5 per 100,000 population[1,2]. Similarly in worldwide, the number of patients is continuously growing annually, which is expected to be ranked as top 3 mortality as of the year 2020[3]. An imbalance between proteolytic and antiproteolytic activity in the lung tissue in response to external stress such as cigarette smoking, or congenital antitrypsin inhibitors appears to be critical for the pathogenesis of major COPD such as emphysema[4-7].

Mundongcheongpye-eum (MCE), also called *Mendongqingfei-yin*, contains eight species of medicinal plants. MCE was known to treat "Feiwei" (肺痿; lung atrophy), a lung disease due to chronic cough, marked by atrophy of the lung with shortness of breath and expectoration[8,9]. This symptoms are similar with them of COPD. Thus, MCE has been an herbal medicine used to treat respiratory diseases such as lung deficiency type of COPD[10]. *Glycyrrhizae Radix* of MCE as licorice flavonoids effectively attenuates lipopolysaccharide (LPS)-induced pulmonary inflammation through the inhibition of inflammatory cell infiltration and inflammatory mediator release which subsequently reduces neutrophil recruitment into lung and neutrophil-mediated oxidative injury[11]. *Ginseng Radix* of MCE improves pulmonary functions and exercise capacity in patients with moderately-severe COPD[12]. *Angelicae Radix* improves on pulmonary hypertension and decreases the level of thromboxane A2 (TXA2) in COPD patients[13].

While clinical evidence strongly suggests the role of MCE in the treatment of lung deficiencies, underlying mechanisms remains to be unexplored. Thus in the present study, possible protective effects of MCE for lung tissues were investigated using in vitro cultured cells and *in vivo* the lung tissues of the experimental mouse model. Lung cells or tissues were exposed to elastase, and possible protection by MCE was explored by biochemical and histochemcial procedures.

Materials and Methods

1. Materials

1) Cell line

A549 cell line, an aneuploid cell line which is derived

* To whom correspondence should be addressed at : Yang Chun Park, Oriental Hospital of Daejeon University, 173-9 Yongdam-dong, Sangdang-gu, Cheongju-si, Chungcheongbukdo, Korea

· E-mail : omdpyc@dju.ac.kr, · Tel : 043-229-3704

· Received : 2010/01/18 · Revised : 2010/09/23 · Accepted : 2010/10/05

from cancerous lung tissue, was obtained from Korean Type Culture Collection (KTCC).

2) Animals

The mice used for the lung disease model were 7-week old male albino ICR (Samtako, Korea). Animals were placed in an animal room with a regulated temperature (22°C), 60% humidity, and a 12 hr light and 12 hr dark cycle. Animals were allowed to eat commercial chow (Samyang Co, Korea) and drink water *ad libitum*.

3) Drug

Mundongcheongpye-eum (MCE), which was purchased from Omni Herb Co (Korea) is a decoction consisting of the following herbal components(Table 1).

Table 1. The Compositions of Mundongcheongpye-eum (MCE)

Herbal medicine	Amount, g (%)
Asteris Radix	8.0 (20.8)
Astragali Radix	6.0 (15.6)
Paeoniae Radix Alba	6.0 (15.6)
Glycyrrhizae Radix	6.0 (15.6)
Ginseng Radix	4.0 (10.4)
Liriopis Tuber	4.0 (10.4)
Angelicae Gigantis Radix	2.4 (6.3)
Schizandrae Fructus	2.0 (5.2)

MCE (76.8 g dry weight) was resuspended in 2 liters of water, heat-extracted with 2 liters of water for 3 hr, and filtered three times. The filtered fluid was distilled using the rotary vacuum evaporator (Büchi 461, Eyela, USA). Concentrated solutions were frozen at -70°C for 4 hr, and freeze-dried for 24 hr. The amount of extracted MCE was 13.7 g showing the yield of 17.8%. The product was kept at 4°C, and dissolved in water. The stock solution (10 ㎎/㎖ in phosphate buffered saline) was stored at -20°C and used for experiment by diluting with physiological saline solution (0.9% NaCl in water) before use.

4) Reagents

Elastase enzyme was purchased from Sigma (USA), dissolved in H_2O, and stored at -80°C until use. Antibodies used in the current study are as follows: anti-elastin rabbit polyclonal antibody (Calbiochem, USA), cleaved caspase 3 (Cell Signalling, USA), fluorescein goat anti-mouse IgG (Invitrogen, USA), rhodamine red-X goat anti-rabbit IgG (Invitrogen, USA), Hoechst 33258 (Invitrogen, USA), anti-cyclin B1 developed in rabbit IgG fraction of antiserum (Sigma, USA), phospho-Erk 1/2 (Cell Signaling, USA), total Erk1/2 (Cell Signaling, USA), actin (MP Biomedicals, USA), goat anti-rabbit IgG-HRP (Santa Cruz Biotechnology, USA).

2. Experimental Procedures

1) In vitro experiments

(1) Cell culture

A549 cells were cultured in RPMI 1640 medium (Lonza, USA) containing 10% heat-inactivated fetal bovine serum (FBS) supplemented with penicillin (100 units/㎖)/streptomycin (100 ㎍/㎖) at 37℃ incubator supplied with 5% CO_2. Activated cells were proliferated at 75 cm^2 flask (SPL, Korea) and transferred every 3 days.

(2) MTT assay

PC12 cell viability was assayed by reduction of MTT[3-(4,5-dimethylthiazole-2-yl)-2,5-diphenyltetrazolium bromide] reagent. Cells (1×10^5/well) were plated in 96-well plate. Cells were treated with 1 unit of elastase and with different concentrations of MCE (0.3 ㎎/㎖ - 1 ㎎/㎖) for 12 hr or 24 hr. Cells were then treated with MTT solution for 4 hr, and optical density was measured using spectrophotometer at 570 ㎚. Cell viability was measured as follows.

$$Cell\ viability = \frac{optical\ density\ of\ cells\ treated\ with\ drugs}{optical\ density\ of\ cells\ treated\ with\ saline\ vehicle} \times 100$$

(3) Immunofluorescence staining

For immunofluorescence staining, A549 cells on the coverslips were fixed with 4% paraformaldehyde, 4% sucrose in phosphate-buffered saline (PBS) at room temperature for 40 min, permeabilized with 0.5% nonidet P-40 in PBS, and blocked with 2.5% horse serum and 2.5% bovine serum albumin for 4 hr at room temperature. Cells on the coverslips were incubated with primary antibody, washed with PBST (PBS plus 0.1% triton X-100) 3 times for 10 min each, and incubated with fluorescein-goat anti-mouse (1:400 dilution, Molecular Probes) or rhodamine-goat anti-rabbit secondary antibodies (Molecular Probes) in 2.5% horse serum and 2.5% bovine serum albumin for 1 hr at room temperature and cover-slipped with gelatin mount medium. For some experimental purpose, Hoechst staining reaction for nuclear visualization was performed between washing steps after secondary antibody reaction (see below for the experimental details of Hoechst staining). The reaction procedures for secondary antibody reaction was performed at the dark place. The merged images were produced by layer blending mode options of the Adobe Photoshop (version 5.5). The primary antibodies used in this study were anti-elastin rabbit polyclonal antibody (1:500, Calbiochem, Germany) and cleaved caspase 3 antibody (1:500, Cell Signaling, USA).

(4) Hoechst staining

Fixed cells on the coverslips were used for Hoechst staining. Hoechst 33258 dye (Sigma, USA) was used to visualize individual cells by staining nucleus. Cells were treated with 25 ㎍/㎖ of Hoechst 33258 in 0.1% triton X-100 in

phosphate-buffered saline solution (PBST) for 10 min. Cell nuclei were visualized blue under the fluorescence microscope.

(5) Western blot analysis

A549 cells were washed with ice-cold phosphate buffered saline (PBS), and sonicated under 50-200 μl of triton lysis buffer (20 mM Tris, pH 7.4, 137 mM NaCl, 25 mM β-glycerophosphate, pH 7.14, 2 mM sodium pyrophosphate, 2 mM EDTA, 1 mM Na_3VO_4, 1% triton X-100, 10% glycerol, 5 ㎍/㎖ leupeptin, 5 ㎍/㎖ aprotinin, 3 μM benzamidine, 0.5 mM DTT, 1 mM PMSF). Protein (15 ㎍) was resolved in 12% SDS polyacrylamide gel and transferred to immobilon polyvinylidenedifluoride (PVDF) membranes (Millipore, USA). Blots were blocked with 5% nonfat dry milk in PBST (17 mM KH_2PO_4, 50 mM Na_2HPO_4, 1.5 mM NaCl, pH 7.4, and 0.05% Tween-20) for 1 hour at room temperature and then incubated overnight at 4℃ in 0.1% triton X-100 in PBS plus 5% nonfat dry milk containing antibodies. Protein bands were detected using the Amersham ECL kit (Amersham Pharmacia Biotech, USA), with horseradish peroxidase-conjugated secondary goat anti-rabbit or goat anti-mouse antibodies (Transduction Laboratories, USA). The antibodies used in the present study were anti-elastin rabbit polyclonal (1:1,000, Calbiochem, Germany), anti-cyclin B1 (1:1,500, Sigma, USA), polyclonal anti-Cdc2 (1:1,500, Santa Cruz, biotechnology, USA), cleaved caspase-3 antibody (1:1,500. Cell Signaling, USA), phospho-p44/42 Erk1/2 kinase antibody (1:4,000, Cell Signaling, USA), p44/42 Erk1/2 kinase antibody (1:4,000, Cell Signaling, USA), actin (1:15,000, MP Biomedicals, USA).

(6) RNA extraction and RT-PCR

① RNA extraction

Cultured PC12 cells were treated and lysed for 10 min with 1 ㎖ of RNAzol^B (easy-BLUE, Intron biotechnology, USA), and 200 μl of chloroform was added, mixed, and phase-separated by centrifugation at 13,000 rpm. Separated upper aqueous phase (400 μl) was recovered, mixed with an equal volume of 2-propanol, and incubated on ice for 15 min. The sample was centrifuged again at 13,000 rpm for 15 min, washed with 80% ethanol, vacuum-dried, and resuspended in 20 μl of diethyl pyrocarbonate (DEPC)-treated water. The amount of isolated RNA was measured by spectrophotomertic measurement of optical density at 260 ㎚. The isolated RNA was denatured at 75℃ and used for the synthesis of the first stranded cDNA.

② RT-PCR

Total RNA was denatured at 75℃ for 5 min and 2.5 μl of 10 mM dNTP mix, 1 ㎍ oligo-dT, 1 μl RNase inhibitor (20 U/μl), 1 μl 100 mM DTT, and 4.5 μl 5×RT buffer (250 mM Tris-HCl, pH 8.3, 375 mM KCl, 15 mM $MgCl_2$), and 1 μl of MMLV RT (200 U/μl) were added to the reaction. PCR was performed using Taq polymerase (Promega, USA) with specific primers for individual reactions. PCR conditions were 94℃ for 5 min of initial DNA denaturation, 94℃ for 30 sec of subsequent denaturation, 55℃ for 30 sec primer annealing, 72℃ for 30 sec polymerization, and 72℃ of 7 min of final polymerization reaction. PCR was usually performed for 30 cycles. The primers used in the present study are listed in Table 2.

Table 2. Nucleotide Sequences used in the Present Study

Target Gene		Primer Sequence	Pruduct Size (bp)
IL-1β	Forward	GCT GAT GGC CCT AAA CAG	672
	Reverse	GAA GAC GGG CAT GTT TTC	
TNF-α	Forward	AGC CCA TGT TGT AGC AAA CC	516
	Reverse	GGT TGA GGG TGT CTG AAG GA	

2) In vivo experiments

(1) COPD animal model

ICR mice (7 weeks old) were inhaled with elastase (0.4 unit in 100 ㎕) and lung injury was observed for 2 days. Animals were randomly assigned into (i) untreated normal group, (ii) control group treated with elastase, and (iii) experimental group treated with elastase and MCE administration (400 ㎎/㎏, *per os*). For elastase injection, animals were lightly anesthetized with 0.05 ㎖ ketamine (50 ㎎/㎖), and elastase solution was inhaled through the nose. MCE were treated for the last 7 days, mice were fasted for 24 hr before sacrifice and then lung tissues were dissected for analysis.

(2) Hemotoxylin & eosin (H & E) staining

The lung tissues were frozen at -20℃ and prepared using cryostat. Sections on slides were immersed in hemotoxylin solution for 1 min and washed several times with running water. Sections were reacted with eosin solution for 1 min and washed again with water, and dehydrated with ethanol series (50%→70%→95%) to remove excess stains on the sections. Finally, slides were mounted with gelatin mount medium and observe under the bright field microscope (Nikon, Japan).

(3) Immunofluorescence staining for lung tissue

For immunofluorescence staining, lung sections on a slide were fixed with 4% paraformaldehyde, 4% sucrose in phosphate-buffered saline (PBS) at room temperature for 40 min, permeabilized with 0.5% nonidet P-40 in PBS, and blocked with 2.5% horse serum and 2.5% bovine serum albumin for 4 hr at room temperature for 16 hr. The remaining part of the immunostaining and Hoechst nuclear staining procedures were essentially the same as for cultured cells.

(4) Western blot analysis for lung tissue

Lung tissue was washed with PBS containing 137 mM NaCl, 2.7 mM KCl, 10 mM Na_2PO_4, 2 mM KH_2PO_4 (pH 7.4), and sonicated under the triton lysis buffer (20 mM Tris, pH 7.4, 137 mM NaCl, 25 mM β-glycerophosphate, pH 7.14, 2 mM sodium pyrophosphate, 2 mM EDTA, 1 mM Na_3VO_4, 1% triton X-100, 10% glycerol, 5 ㎍/㎖ leupeptin, 5 ㎍/㎖ aprotinin, 3 μM benzamidine, 0.5 mM DTT, 1 mM PMSF). The amount of protein in each lysate was quantitated by spectrophotometer, and 15 ㎍ of protein was used for SDS-polyacrylamide gel electrophoresis. The remaining procedure for western analysis was essentially same as described above.

(5) Microscopic analysis

Images from immunofluorescence staining were analyzed by fluorescence microscope (Nikon, Japan) and those from H & E staining were analyzed by bright-field and phase contrast microscope. The images were captured and transferred into the computer software (ACT-1). Merged images were analyzed under the image blend mode of the Photoshop software (version 5.5).

3) Statistical analysis

Data were presented as mean±standard error of mean (SEM). A StatView512+^{TM} computer software was used for statistical analysis by one way ANOVA. The p-value less than 0.05 was considered as statistically significant.

Results

1. *In vitro*

1) Effects of MCE on the survival of elastase-treated cells

To investigate the effects of MCE on the survival of elastase-treated cells, cell viability was determined by MTT assay. A percentage of cell survival was in the range between 95% and 102% when the cells were treated with 0.01 ㎎/㎖ and up to 1.0 ㎎/㎖ of MCE(Fig. 1A). Cell survival was further examined after treatment of elastase with different concentrations of MCE. Cell survival was significantly decreased by elastase treatment for 12 hr or 24 hr, and additional treatment of MCE at 0.3 ㎎/㎖ to 1.0 ㎎/㎖ significantly elevated cell survival. The data further showed that MCE at the concentration of 0.3 ㎎/㎖ to 0.5 ㎎/㎖ was appropriate to recover cell survival, and these two concentrations were used for the remaining of the current study(Fig. 1B)

2) Effects of MCE on the elastin protein levels

Elastin protein levels were examined in A549 cells after elastase and MCE treatments. Elastase treatment for 12 hr or 24 hr decreased elastin protein levels in A549 cells. However, when the cells were treated with MCE together with elastase, elastin protein levels maintained similar to those of untreated control cells(Fig. 2A).

To investigate the integrity of A549 cells, cultured A549 cells were used for immunofluorescence staining for elastin protein. When A549 cells were treated with elastase for 12 hr or 24 hr, it was observed that elastin protein signals were observed to levels similar to those of the intact control, but, in many of stained cells, the signals were localized more centrally, particularly in cells with 24 hr treatment of elastase. This pattern of signaling displacement was much reduced when the cells were treated with MCE in addition to elastase(Fig. 2B). Merged images of nuclear signals with elastin protein in cells treated elastase showed overall overlapping in nuclear area whereas in cells treated with elastase and MCE, elastin was localized in perinuclear area in addition to nuclear area(Fig. 2C).

3) Effects of MCE on A549 cell death by elastase treatment

To determine whether apoptotic signaling pathway is involved in elastase-mediated cell death, changes in caspase 3 protein levels in A549 cells were tested. In the intact A549 cells, no caspase 3 protein signals were detected, but the treatment of elastase for 12 hr or 24 hr clearly induced caspase 3-positive cells(Fig. 3A). The number of caspase 3-positive cells were much more increased in cells treated with elastase for 24 hr than those with 12 hr. MCE addition decreased caspase 3-positive cells in A549 cells with 12 hr or 24 hr treatment with elastase. It was further observed that in A549 cells treated with elastase and MCE for 24 hr, caspase 3-positive cells revealed nuclear morphology with shrunken and/or fragmented pattern(Fig. 3B).

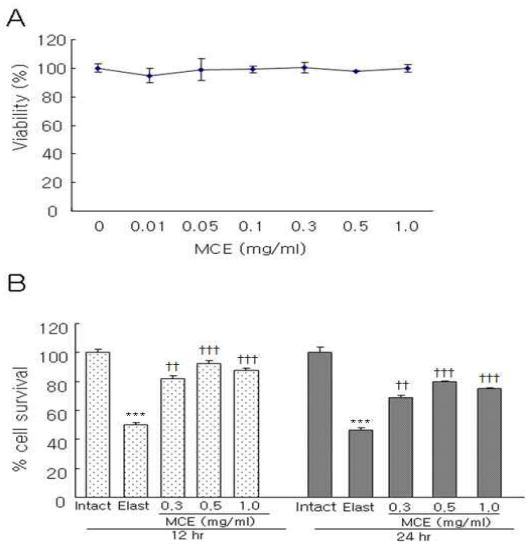

Fig. 1. MTT assay of A549 cells to determine cell viability. (A) A549 cells were treated with different concentrations of MCE for 24 hr and harvested for MTT assay. (B) A549 cells were treated with elastase (1 unit) alone or in the presence of 0.3-1.0 ㎎/㎖ of MCE. ***: p<0.001 compared to control by ANOVA test ††: p<0.01 †††: p<0.001 compared to elastase by ANOVA test.

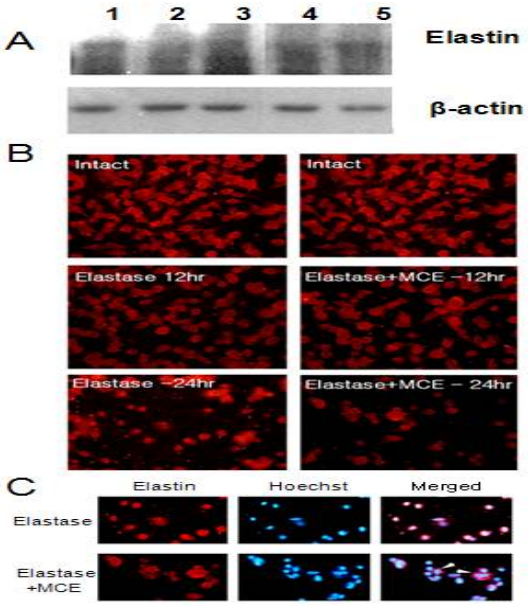

Fig. 2. Changes of elastin protein levels in A549 cells by MCE treatment. (A) Western blot analysis for actin protein was performed as an internal loading control. Lanes 1: intact control, 2: elastase (1 unit) 12 hr, 3: elastase (1 unit) 24 hr, 4: elastase (1 unit) plus MCE (0.5 ㎎/㎖) 12 hr, 5: elastase (1 unit) plus MCE (0.5 ㎎/㎖) 24 hr. (B) A549 cells were analyzed by immunofluorescence staining for elastin protein. (C) Merged view of elastin protein signals (red) in A549 cells with Hoechst nuclear staining (blue). Perinuclear elastin protein signals in cells treated with elastase and MCE for 24 hr were indicated by arrowheads.

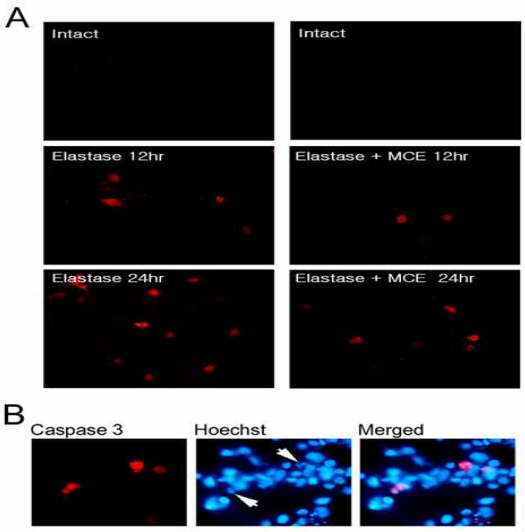

Fig. 3. Identification of caspase 3-positive cells in A549 cells after elastase and MCE treatments. (A) Immunofluorescence staining of A549 cells with anti-caspase 3 antibody and MCE. Caspase 3-positive cells were identified in red color. (B) Nuclear identification of caspase 3-positive cells. A549 cells were treated with elastase and MCE for 24 hr and used for caspase 3 immunostaining (red) and Hoechst nuclear staining (blue). The nuclei positive to caspase 3 were marked by arrows in Hoechst-stained image.

4) Effects of MCE on Cdc2 and cyclin B1 signaling pathways in A549 cells

To determine the effects of MCE treatments on cell proliferation, Cdc2 and cyclin B1 protein levels were investigated in elastase-treated A549 cells. Elastase treatment slightly decreased Cdc2 protein levels, and 24 hr treatment further decreased Cdc2 protein levels. MCE treatment for 12 hr did not change compared to those treated with elastase, but MCE treatment for 24 hr increased Cdc2 levels compared to 24 hr elastase-treated control. Cyclin B1 protein levels were barely detected in untreated control cells and elastase-treated cells. However, cyclin B1 protein was strongly detected in elastase-treated A549 cells with MCE for 12 hr and 24 hr(Fig. 4).

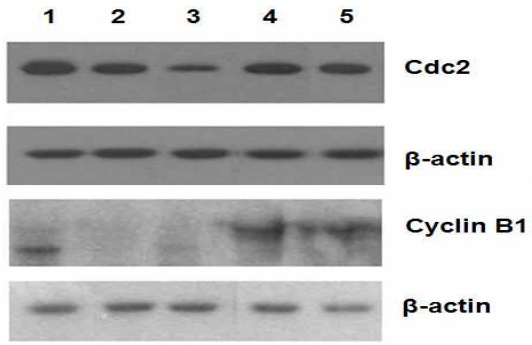

Fig. 4. Changes of cell cycle protein levels in A549 cells by MCE treatment. A549 cells were cultured and treated with elastase or elastase plus MCE for 12 hr or 24 hr. Cell lysate was used for western blot analysis with anti-Cdc2 antibody and anti-cyclin B1 antibody. Western blot analysis for actin protein was performed as an internal loading control. Lanes 1: intact control, 2: elastase (1 unit) for 12 hr, 3: elastase (1 unit) for 24 hr, 4: elastase (1 unit) plus MCE (0.5 ㎎/㎖) for 12 hr, 5: elastase (1 unit) plus MCE (0.5 ㎎/㎖) for 24 hr.

5) Effects of MCE on Erk1/2 activity in A549 cells

To examine the effects of MCE treatment on elastase-treated A549 cells, Erk1/2 protein activity was investigated by measuring phospho-Erk1/2 protein levels. Basal levels of phospho-Erk1/2 protein were detected in untreated control cells, and some decreases in phospho-Erk1/2 levels were observed after elastase treatment for 24 hr. When MCE was treated for 12 hr, phospho-Erk1/2 was not altered, but after 24 hr treatment, obvious increased phospho-Erk1/2 protein was detected(Fig. 5).

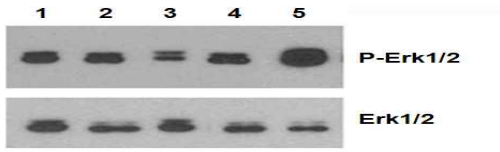

Fig. 5. Changes of phospho-Erk1/2 and total Erk1/2 protein levels in A549 cells by MCE treatment. A549 cells were cultured and treated with elastase or elastase plus MCE for 12 hr or 24 hr. Cell lysate was used for western blot analysis for phospho-Erk1/2 and total Erk1/2 proteins. Western blot analysis for Erk1/2 protein was performed as an internal loading control. Lanes 1: intact control, 2: elastase (1 unit) 12 for hr, 3: elastase (1 unit) for 24 hr, 4: elastase (1 unit) plus MCE (0.5 ㎎/㎖) for 12 hr, 5: elastase (1 unit) plus MCE (0.5 ㎎/㎖) for 24 hr.

6) Effects of MCE on expression of inflammatory cytokines in A549 cells

To determine whether elastase treatment induce mRNA

expression of IL-1β and TNF-α in A549 cells with different treatments, RNA from A549 cells was used for RT-PCR analysis. IL-1β and TNF-α mRNA induction slight increased in A549 cells treated with elastase for 12 hr and further elevated by 24 treatment of elastase. MCE treatment for 12 hr or 24 hr attenuated IL-1β and TNF-α mRNA levels in A549 cells(Fig. 6).

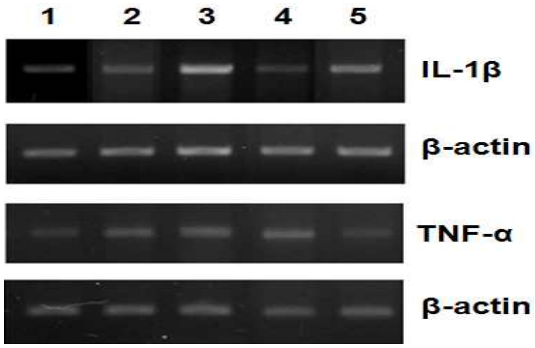

Fig. 6. RT-PCR analysis of IL-1β and TNF-α mRNA expression in A549 cells. After various treatments, RNA was isolated from each experimental group and was used for RT-PCR. Amplified DNA of IL-1β TNF-α were detected at expected size position (IL-1β; 672 bp). RT-PCR for actin mRNA (DNA band size; 409 bp) was performed as an internal loading control. Lanes 1: intact control, 2: elastase (1 unit) for 12 hr, 3: elastase (1 unit) for 24 hr, 4: elastase (1 unit) plus MCE (0.5 ㎎/㎖) for 12 hr, 5: elastase (1 unit) plus MCE (0.5 ㎎/㎖) for 24 hr.

2. In vivo

1) Effects of MCE on histological analysis of lung tissue

The effects of elastase and MCE treatment on lung tissue were investigated by H & E histological staining and Hoechst nuclear staining. Many of the small sizes of alveoli were observed in the lung tissue from untreated control animal. However, greatly dilated alveoli were frequently observed in the lung tissue treated with elastase. When the animals were administered with MCE in addition to elastase, the sizes of alveoli were similar to those in untreated control animals(Fig. 7A). In elastase-treated tissue, enlarged form of aggregated cells were observed around the alveoli(Fig. 7B). Lung tissue sections from the intact control mouse and the mice treated with elastase or elastase plus MCE were used for Hoechst nuclear staining. While individual nuclei were observed evenly throughout the intact lung tissue, heavily localized staining pattern was observed around some of the enlarged alveoli in elastase-treated group. In tissue from elastase plus MCE treatments, nuclear distribution was very similar to those of the intact control tissue(Fig. 7C).

2) Effects of MCE on elastin protein in the lung tissue

Elastin protein levels and its distribution in the lung tissue were investigated by western and immunofluorescence staining analyses. To examine elastin protein levels quantitatively, lung tissues were subjected to western blot analysis. Elastase treatment decreased elastin protein, compared with intact control. MCE treatment resulted in elevated elastin protein expression(Fig. 8A). Immunofluorescence staining of elastin protein in the intact lung tissue showed that intense protein signals were particularly found around the alveoli(Fig. 8B). Elastin signals were greatly decreased in elastase-treated tissue, but the signal intensities were elevated by MCE treatment(Fig. 8B).

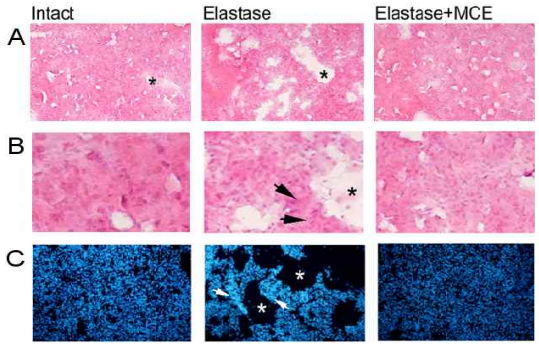

Fig. 7. Histological analysis of lung tissues from mice after different treatments. Mice after different treatments, lung tissue was dissected out and the sections were used for H & E cytological staining. (A) The areas shown white indicate alveoli (marked asterisks). (B) Enlarged images for the stained lung tissue. Notice strong eosinophilic staining around the alveolus in elastase-treated group (arrows). In (A) and (B), tissue sections were analyzed under the bright-field microscope (A: 200×magnification, B: 400×magnification). (C) Hoechst nuclear staining analysis of lung tissues from mice after different treatments. Mice after different treatments, lung tissue was dissected out and the sections were used for nuclear staining with Hoechst 33258. The sections were analyzed under the fluorescence microscope (200×magnification). The alveolar areas were marked by asterisks, and the arrow at the vicinity to the alveoli showed strongly stained nuclei in the elastase-treated group.

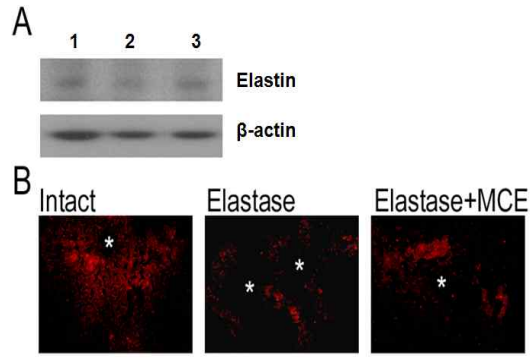

Fig. 8. Analysis of elastin protein in lung tissue after different treatment. Lung tissue after different treatment was dissected and used for western analysis (A) and for immunofluorescence staining (B). Western blot for actin protein was performed as an internal loading control. In (B), the area of alveolus was marked by asterisk and stronger elastin signals were seen the adjacent area to the alveoli. lane 1; untreated intact control, lane 2; elastase treated, lane 3; elastase plus MCE treated.

3) Effects of MCE on Cdc2 and cyclin B1 protein levels in lung tissue

To determine possible changes in cell proliferation in the lung, Cdc2 proteins levels were analyzed by western blot analysis. Cdc2 protein was barely detected in the intact lung tissues and slightly increased after elastase treatment. MCE

treatment in addition to elastase treatment induced strong increases in Cdc2 protein levels(Fig. 9A). Cdc2 regulatory protein cyclin B1 protein levels were similar between three experimental groups though some non-specific bands interfered for the detection sensitivity(Fig. 9B). Tissue distribution of Cdc2 protein signals was analyzed by immunofluorescence staining.

Cdc2 protein of the elastase treated tissues relatively increased than intact control. Enhanced Cdc2 signals were seen in the lung tissue treated with elastase plus MCE, as observed by western analysis(Fig. 9C). Cyclin B1 protein signals were observed constitutively in the intact lung tissue and heavily localized, intense signaling was seen in elastase-treated tissue. Tissue distribution of cyclin B1 signals after MCE treatment was similar to that in the intact tissue. However, overall levels of protein signals were similar among 3 experimental groups, as has been observed by western blot analysis(Fig. 9D).

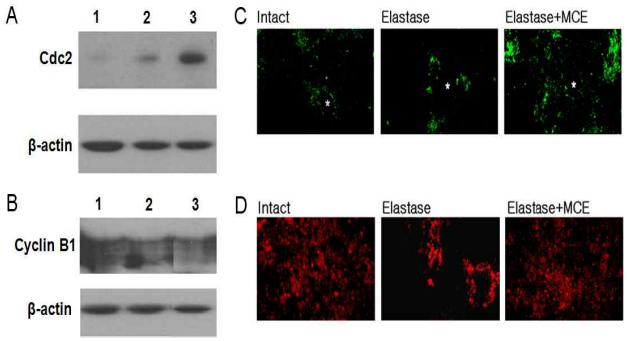

Fig. 9. Cdc2 and cyclin B1 protein analysis in lung tissue after different treatment. Lung tissue after different treatment was dissected and used for western analysis for Cdc2 and cyclin B1. Western analysis for actin protein was performed as an internal loading control (A and B). Lane 1; untreated intact control, lane 2; elastase treated, lane 3; elastase plus MCE treated. Cdc2 and cyclin B1 protein signals in the lung tissue from intact, elastase-treated, and elastase plus MCE-treated mice. Lung tissue was used for immunofluorescence staining for the detection of Cdc2 (green) and cyclin B1 (red) protein signals (C and D).

4) Effects of MCE on phospho-Erk1/2 protein levels in lung tissue

Changes in survival activity of lung cells was investigated by MCE administration. Quantitative analysis of phospho-Erk1/2 in the lung tissue showed a low level of Erk1/2 activity in untreated normal tissue. Elastase treatment increased phospho-Erk1/2 levels, and MCE administration further elevated. Total Erk1/2 levels which were produced moderately were not changed by different treatments(Fig. 10A). To determine subcellular localization of induced phospho-Erk1/2 in the lung tissue, immunofluorescence staining for phospho-Erk1/2 protein was performed. Phospho-Erk1/2 signals were more intense in elastase-treated tissues compared to intact control(Fig. 10B). When MCE was treated in elastase-treated animal, phospho-Erk1/2 signal was further enhanced. To investigate subcellular distribution of phospho-Erk1/2 signals, fluorescence view of phospho-Erk1/2 was merged with Hoechst-stained nuclei. Phospho-Erk1/2 signals were largely overlapped with nucleus areas, and some additional signals were found in the perinuclear area(Fig. 10C).

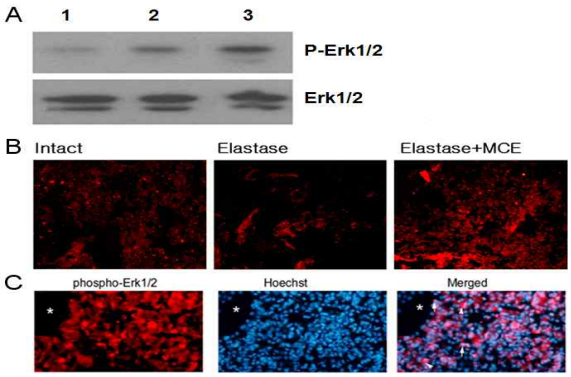

Fig. 10. Analysis of phospho-Erk1/2 protein signals in the lung tissue. (A) Protein lysates from the lung tissue were used for western analysis, and the analysis for Erk1/2 was performed as an internal loading control. Lane 1; untreated intact control, lane 2; elastase treated, lane 3; elastase plus MCE treated. Analysis of phospho-Erk1/2 protein signals in the lung tissue. (B) Phospho-Erk1/2 signals were compared among the lung tissue with different treatments (in red). (C) Immunofluorescence view of phospho-Erk1/2 images with Hoechst-stained nuclei. The lung tissue treated with elastase and MCE was used for immunofluorescence staining. In the merged image, the arrow indicates phospho-Erk1/2 signals found in the nuclear area and the arrowheads shows phospho-Erk1/2 signals surrounding perinuclear cytoplasmic zone.

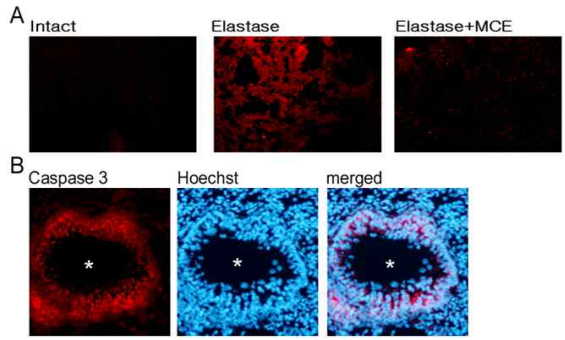

Fig. 11. Immunofluorescence staining analysis of caspase 3 protein signals in the lung tissue after different treatments. (A) Caspase 3 protein signals was detected in red under the fluorescence microscopic analysis. (B) Merged images of caspase 3 protein signals (in red) with Hoechst-stained nuclei (blue). Notice heavily stained caspase 3 signals surrounding the alveolus (marked asterisk) in the lung tissue which had been prepared from the animals administered with elastase.

5) Effects of MCE on caspase 3 protein levels in lung tissue

Possible involvement of apoptotic cell death was investigated by immunofluorescence staining in the lung tissue. In the intact lung tissue, caspase 3 protein signals were not detected, but clear signals were found after elastase treatment(Fig. 11A). When treated with MCE in addition to elastase, caspase 3 protein signals were largely attenuated in the lung cells. Merged image of caspase 3 fluorescence view

with Hoechst-nuclei revealed that relatively stronger signals were positioned around the alveoli in the elastase-treated lung tissue(Fig. 11B).

Discussion

COPD is a disease state characterized by airflow limitation that is not fully reversible. The airflow limitation is usually both progressive and associated with an abnormal inflammatory response of the lungs to noxious particles or gases[14]. Although pathological genesis for COPD is not fully understood, studies suggested that the two imbalances are protease-antiprotease imbalances and oxidant-antioxidant imbalance[15]. Smoking, for instance, can increase neutrophil's elastase levels in the blood, which is to attack lung tissue[16].

In oriental medicine, MCE is known to treat lung symptoms such as chronic cough, which might be associated with COPD. Moreover, it was reported that some of herbal components such as Glycyrrhizae Radix and Ginseng Radix are effective for protecting lung tissues from inflammatory damages[11,12]. However, possible mechanism underlying its effects on respiratory diseases have not been studied at cellular and molecular levels. Therefore in the current study, cellular factors which are known to be important for survival or death were investigated using cultured cells and in vivo lung tissues in an experimental mouse model.

Unregulated elastase activity in the lung tissue can cause the loss of elastic recoil, which is accompanied by destruction of bronchioles and alveolar walls. Consequently, the dilation of the alveolar ducts might result in inefficient ventilation and perfusion inequalities. As an experimental animal models for COPD, the animal was given external inflammatory stress for example instilling papain, a plant inhibitor, cigarette smoking[17]. To examine more specific target molecules, transgenic mouse overexpressing metalloprotease I or interferon-gamma, or knockout mouse approaches were developed[18,19].

In the present study, investigations on the molecular factors in relation to emphysema were studied using in vitro cultured cells (A549 epithelial cell line) and in vivo mouse model. A549 cell line is derived from the epithelium of the lung cancer tissue, and, together with BEAS-2B cells, is widely used for molecular studies on lung diseases[17,20]. When A549 cells were treated with elastase, cell damage was clearly observed by morphological, biochemical, and function (metabolic) criteria. Treatment of A549 cells with elastase for 12 hr to 24 hr induced cell death responses. Elastase activity on A549 cells were well observed by elastin-stained cells: after 24 hr treatment with elastase, cells tend to be shrunken to be a round shape. Since elastin is a fibrous protein to provide resilience of the cell or tissue structure, its degradation could collapse the periplasmic integrity of the cell. When MCE was treated to A549 cells together with elastase, elastin-labeled cell morphology was more similar to untreated control cells rather than elastase-treated cells, suggesting possible protection of elastin structures by MCE.

Treatment of A549 cells by elastase activated, to a certain extent, the apoptotic cell death pathway, as identified by positive caspase 3 signals. Caspase 3 positive cells were clearly observed and increased after elastase treatment up to for 24 hr. Caspase 3 is one of critical proteases which is activated during the apoptotic cell death process[21]. Caspase 3 activates substrate proteins such as DNA degradation enzymes and important cytoskeletal proteins, suggesting that elastase-treated A549 cells may involve apoptosis cell death pathway[20]; however, it should be noted that many of dying cells did not show caspase 3-positive signals, suggesting that both apoptotic and necrotic cell death pathway might be involved in A549 cells treated with elastase.

When the mouse was inhaled with elastase through nasal inhalation, in the lung tissue, increased cell population around the alveoli and enlarged airspaces distal to the terminal bronchi were observed[22]. This histological feature could be associated with pathological pattern of emphysema. Indeed, imbalance of elastase activity and oxidation-reduction have been implicated to cause emphysema[23]. Elastin protein play an important role for the integrity of acinar structures by maintaining eleatic recoil which is to support alveolar space against transmural pressure toward intrapleural space[24,25]. When there is a defect in elastin, alveolar duct area is expanded, showing pathological features of emphysema.

Elastase-treated lung tissue showed increased signals of caspase 3 proteins around the alveolar ductal area, suggesting that apoptotic cell death are commonly involved in A549 cells and in vivo lung tissue. These data further implicate that both in vitro and in vivo experimental paradigms may be useful to investigate emphysema and complement each other.

Treatment of MCE into elastase-treated A549 cells and lung tissue appeared to recover cell and tissue morphology similar to untreated controls, and major findings are described as follows. First, MCE treatment changed elastin-labeled A549 cells which was condensed, round shape into fibrous shape. Second, in vivo alveolar airspace was reduced and adjacent dense cell population was decreased. Third, the number of caspase 3-positive cells was largely reduced to a similar level as untreated control. Together, these data suggest that MCE

appears to mediate protection of elastase-treated lung's epithelial cells or lung's epithelial cell lines.

Selected molecular candidates that might be involved in cell or tissue damages by elastase and possible protection by MCE were further investigated. First, Erk1/2 protein kinase as a principal mitogen activated protein (MAP) kinase family proteins was investigated. Erk1/2 indicates two Erk family proteins Erk1 and 2, both of which have very similar molecular size (42 and 44 kDa) and share major biochemical properties. Erk family proteins, together with p38 and c-Jun N-terminal kinase (JNK), comprises of MAP kinase proteins. These proteins are known to be activated by upstream kinase such as MEK family proteins, which is activated by another upstream kinase called MEKK proteins[26,27]. Many of the MAP kinase family proteins are constitutively expressed in the cells and can be activated by phosphorylation by upstream kinases. For instance, Erk1/2 is produced in normal situation, but can be activated by phosphorylation by MEK1/2 in responses to external stimulation. Once activated, these kinases phosphorylate downstream substrate proteins; for instance in many cells, Erk1/2 phosphorylates MEF2C and cAMP responsive element binding protein (CREB) which can act transcription factors for the induction of gene expression[28,29]. Since activation pathways and downstream target proteins among these proteins are cross-linked each other in many cases, their cell biological functions are not defined in a distinct manner. Yet, several lines of experimental data strongly implicated that Erk1/2 activation is important for inducing cell survival, differentiation and proliferation whereas activation of JNK and p38 are more important for the induction of apoptotic cell death pathway[30].

In the present study, elastase treatment of A549 cells resulted in decreased levels of phospho-Erk1/2 which could be functionally related to cell injury and death. However, Erk1/2 activity, which was barely observed in the normal lung tissue, was increased after elastase treatment. One possible interpretation of this discrepancies would be that normal A549 cells in culture may require a certain level of Erk1/2 activity for their survival and continuous proliferation in the culture condition. In contrast, the lung cells in normal animals may not require such an active cellular activity. When A549 cells are treated with elastase, cell damage and decreased cellular activity could be positively related with decreased Erk1/2 activity. However in elastase-treated lung cells, cellular activity that tries to survive against elastase-induced injury signals could be induced and this can rather increase Erk1/2 activity; this interpretation is consistent with a previous report[31] and the increased number of Hoechst-stained nuclei around the alveolar space in elastase-treated animal. This difference in the interpretation is based on the structural integrity between cells and tissue in responses against external insults, which could result in opposite consequences: irresistible damage response vs resistable survival activity.

Interestingly however, Erk1/2 activity was increased by MCE treatment in both cases, which supporting the idea that MCE may elevate survival activity in damaged cells. How MCE-induced Erk1/2 activity is functionally related to lung cell protections against elastase-induced insults remains to be explored. Identification of phospho-Erk1/2 signals in lung tissue by immunofluorescence staining showed the existence of the protein signals in the perinuclear as well as nuclear areas, suggesting that phospho-Erk1/2 might have target substrates in both cytoplasm and nucleus. Transcription factor such as CREB could be activated by phosphorylation by Erk1/2 and induce target gene expression.

As one of the ways to determine increased cellular proliferation in MCE-treated lung cells against elastase treatments, changes in Cdc2 and its regulatory protein cyclin B1 were investigated in A549 cells and lung tissues. Cdc2, also called cyclin-dependent kinase 1 (Cdk1), is the prototypical Cdk family protein which is known to be critical for cell cycle progression[32-34]. Although activation of Cdc2 is important for the transition of G2 (growth phase 2) to M (mitosis) phase while other Cdk family proteins such as Cdk2 is more important for G1 to S phase transition, recent study suggests that Cdc2 alone is sufficient for whole cell cycle progression[35]. Cdc2 activation requires the binding of regulatory protein cyclin B protein; Of two different cyclin proteins B1 and B2, cyclin B1 is more important for cell cycle progress and cyclin B2 may function more important for cytoskeletal rearrangement during cell motility[36]. Thus, regular progression of cell cycle requires Cdc2 kinase activity which is fulfilled by Cdc2 and cyclin B1.

It has been primarily observed in this study that the number of nuclei of cultured A549 cells and lung cells were decreased by elastase treatment and elevated similar to the normal levels by MCE treatment, strongly suggesting that MCE treatment activated cell cycle progression as one of the ways to protect the cells from external insults, raising the possible involvement of cell cycle machinery. In A549 cells, both Cdc2 and cyclin B1 levels were decreased after elastase treatment, and cyclin B1, but not Cdc2 protein, levels were elevated by MCE treatment. In contrast in lung tissue, cyclin B1 protein, but not Cdc2, protein levels were unregulated after MCE treatment. Thus, possible mechanism in regulating cell cycle progression by MCE treatment seems to be operated in

different manner between A549 cells and lung cells. In any case, increased Cdc2 activity as protein kinase would be expected, and increased cell proliferation would be resulted in both cases.

As one of the ways to investigate general pathological mechanism, changes in mRNA expression of TNF-α and IL-1β were investigated. These two proteins are the representative inflammatory cytokines that are known to be strongly induced in most of the acute inflammatory reactions[37,38]. To investigate whether TNF-α and IL-1 β induction are regulated at the gene expression levels, RT-PCR was performed in both A549 cells and lung tissues. In both cases, TNF-α and IL-1 mRNA levels were increased after elastase treatment, implicating increased production of IL-1β and TNF-α proteins in affected cells. MCE treatment into the corresponding cells resulted in decreased levels of mRNA for both proteins. Thus, elastase treatment appears to involve inflammatory responses which is alleviated by MCE treatment(Fig. 12). Further studies on dosage and modified prescriptions are warranted.

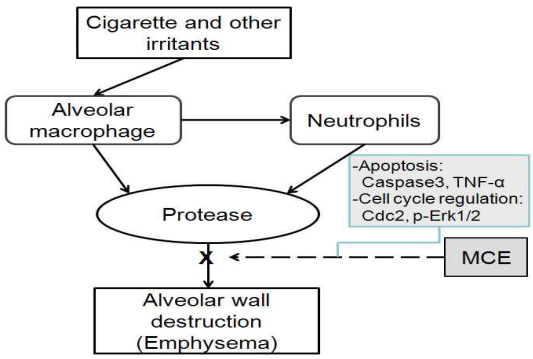

Fig. 12. Role of protease on pathogenesis of COPD and target of MCE.

Conclusion

The present study was performed to investigate whether MCE has protective role for lung cells which had been treated with elastase. As experimental system, both cultured A549 cells and in vivo lung tissue were investigated by histological and biochemical approaches. The major findings are summarized as follows.

MCE significantly increased cell survival rate in MTT assay and protected lung tissue injury in morphological examinations. MCE increased Cdc2 activity in both cultured A549 cells and in vivo lung tissue. MCE increased phospho-Erk1/2 activity in both cultured A549 cells and in vivo lung tissue. MCE inhibited caspase 3 activity in both A549 cells and in vivo lung tissue, but largely inhibited by MCE treatment. MCE suppressed the expression levels of inflammatory cytokine proteins IL1-β and TNF-α in cultured A549 cells.

Taken together, MCE treatment appears to regulate pathophysiological responses by elastase treatment in lung cells. Furthermore, MCE effects seems to act on the target cells in diverse manner. Further studies on the characterization of diverse molecular components in MCE would be helpful to delineate pathophysiological observations into molecular mechanism.

Acknowledgments

This research was supported by Basic Science Research Program through the National Research Foundation of Kore (NFR) funded by the Ministry of Education, Science and Technology (2010-0010960)

References

1. Korea National Statistical Office, Republic of Korea [Internet]. Dajeon: Korea National Statistical Office; c1996-[cited 2009 Mar]. Available from: http://www.nso.go.kr
2. Kim, D.S., Kim, Y.S., Jung, K.S., Chang, J.H., Lim, C.M., Lee, J.H. Prevalence of chronic obstructive pulmonary disease in Korea: a population-based spirometry survey. Am J Respir Crit Care Med. 172(7):842-847, 2005.
3. Lopez, A.D., Murray, C.C. The global burden of disease, 1990-2020. Nat Med. 4(11):1241-1243, 1998.
4. Churg, A., Wright, J.L. Proteases and emphysema. Curr Opin Pulm Med. 11(2):153-159, 2005.
5. Ioachimescu, O.C., Stoller, J.K. A review of alpha-1 antitrypsin deficiency. COPD. 2(2):263-275, 2005.
6. Stoller, J.K., Aboussouan, L.S. Alpha1-antitrypsin deficiency. Lancet. 365(9478):2225-2236, 2005.
7. Tremblay, G.M., Janelle, M.F., Bourbonnais. Y. Anti-inflammatory activity of neutrophil elastase inhibitors. Curr Opin Investig Drugs. 4(5):556-565, 2003.
8. Hur, J. Dongeuibogam. Seoul, Namsandang, pp 481-482, 1989.
9. World Health Organization. WHO International Standard Terminologies on Traditional Medicine in the Western Pacific Region. Geneva, World Health Organization, p 176, 2007.
10. Committee of Oriental Respiratory Medicine. Oriental Internal Medicine of Lung System. Seoul, Gukjin, pp 338-346, 2004.
11. Xie, Y.C., Dong, X.W., Wu, X.M., Yan, X.F., Xie, Q.M.

Inhibitory effects of flavonoids extracted from licorice on lipopolysaccharide-induced acute pulmonary inflammation in mice. Int Immunopharmacol. (2):194-200, 2009.

12. Gross, D., Shenkman, Z., Bleiberg, B., Dayan, M., Gittelson, M., Efrat, R. Ginseng improves pulmonary functions and exercise capacity in patients with COPD. Monaldi Arch Chest Dis. 57(5-6):242-246, 2002.
13. Zheng, L. Short-term effect and the mechanism of radix Angelicae on pulmonary hypertension in chronic obstructive pulmonary disease. Zhonghua Jie He He Hu Xi Za Zhi. 15(2):95-97, 1992.
14. Pauwels, R.A., Buist, A.S., Calverley, P.M., Jenkins, C.R., Hurd, S.S.; GOLD Scientific Committee. Global strategy for the diagnosis, management, and prevention of chronic obstructive pulmonary disease. NHLBI/WHO Global Initiative for Chronic Obstructive Lung Disease (GOLD) Workshop summary. Am J Respir Crit Care Med. 163(5):1256-1276, 2001.
15. Macnee, W. Pathogenesis of chronic obstructive pulmonary disease. Clin Chest Med. 28(3):479-513, 2007.
16. Shapiro, S.D. Evolving concepts in the pathogenesis of chronic obstructive pulmonary disease. Clin Chest Med. 21(4):621-632, 2000.
17. Marwick, J.A., Kirkham, P., Gilmour, P.S., Donaldson, K., MacNEE, W., Rahman, I. Cigarette smoke-induced oxidative stress and TGF-beta1 increase p21waf1/cip1 expression in alveolar epithelial cells. Ann N Y Acad Sci. 973: 278-283, 2002.
18. Dawkins, P.A., Stockley, R.A. Animal models of chronic obstructive pulmonary disease. Thorax. 56(12):972-977, 2001.
19. Cawston, T., Carrere, S., Catterall, J., et al. Matrix metalloproteinases and TIMPs: properties and implications for the treatment of chronic obstructive pulmonary disease. Novartis Found Symp. 234: 205-218, 2001.
20. Nakajoh, M., Fukushima, T., Suzuki, T., et al. Retinoic acid inhibits elastase-induced injury in human lung epithelial cell lines. Am J Respir Cell Mol Biol. 28(3):296-304, 2003.
21. Kroemer, G., Martin, S.J. Caspase-independent cell death. Nat Med. 11(7):725-730, 2005.
22. Fukuda, Y., Kawamoto, M., Yamamoto, A., Ishizaki, M., Basset, F., Masugi, Y. Role of elastic fiber degradation in emphysema-like lesions of pulmonary lymphangiomyomatosis. Hum Pathol. 21(12):1252-1261, 1990.
23. Karlinsky, J., Fredette, J., Davidovits, G., et al. The balance of lung connective tissue elements in elastase-induced emphysema. J Lab Clin Med. 102(2):151-162, 1983.
24. Kononov, S., Brewer, K., Sakai, H., et al. Roles of mechanical forces and collagen failure in the development of elastase-induced emphysema. Am J Respir Crit Care Med. 164(10 Pt 1):1920-1926, 2001.
25. Stone, P.J., Calore, J.D., McGowan, S.E., Bernardo, J., Snider, G.L., Franzblau, C. Functional alpha 1-protease inhibitor in the lower respiratory tract of cigarette smokers is not decreased. Science. 221(4616):1187-1189, 1983.
26. Davis, R.J. Signal transduction by the JNK group of MAP kinases. Cell. 103(2):239-252, 2000.
27. Weston, C.R., Davis, R.J. The JNK signal transduction pathway. Curr Opin Genet Dev. 12(1):14-21, 2002.
28. Bozon, B., Kelly, A., Josselyn, S.A., Silva, A.J., Davis, S., Laroche, S. MAPK, CREB and zif268 are all required for the consolidation of recognition memory. Philos Trans R Soc Lond B Biol Sci. 358(1432):805-814, 2003.
29. Whitmarsh, A.J., Davis, R.J. Structural organization of MAP-kinase signaling modules by scaffold proteins in yeast and mammals. Trends Biochem Sci. 23(12):481-485, 1998.
30. Xia, Z., Dickens, M., Raingeaud, J., Davis, RJ., Greenberg, M.E. Opposing effects of ERK and JNK-p38 MAP kinases on apoptosis. Science. 270(5240):1326-1331, 1995.
31. Mercer, B.A., D'Armiento, J.M. Emerging role of MAP kinase pathways as therapeutic targets in COPD. Int J Chron Obstruct Pulmon Dis. 1(2):137-150, 2006.
32. Moreno, S., Nurse, P. Substrates for p34cdc2: in vivo veritas? Cell. 61(4):549-551, 1990.
33. Nurse, P. Universal control mechanism regulating onset of M-phase. Nature. 344(6266):503-508, 1990.
34. Pines, J., Hunter, T. Cyclin-dependent kinases: a new cell cycle motif? Trends Cell Biol. 1(5):117-121, 1991.
35. Goga, A., Yang, D., Tward, A.D., Morgan, D.O., Bishop, J.M. Inhibition of CDK1 as a potential therapy for tumors over-expressing MYC. Nat Med. 13(7):820-827, 2007.
36. Pines, J. Cyclins: wheels within wheels. Cell Growth Differ. 2(6):305-310, 1991.
37. Ruddle, N.H. Tumor necrosis factor (TNF-alpha) and lymphotoxin (TNF-beta). Curr Opin Immunol. 4(3):327-332, 1992.
38. Ruuls, S.R., Sedgwick, J.D. Cytokine-directed therapies in multiple sclerosis and experimental autoimmune encephalomyelitis. Immunol Cell Biol. 76(1):65-73, 1998.